01 Jan 2004

using Near-Field Scanning to Predict Radiated Fields

Jin Shi

Michael A. Cracraft

Jianmin Zhang

Richard E. DuBroff
Missouri University of Science and Technology, red@mst.edu

et. al. For a complete list of authors, see *https://scholarsmine.mst.edu/ele_comeng_facwork/1932*

Recommended Citation

J. Shi et al., "using Near-Field Scanning to Predict Radiated Fields," *Proceedings of the InternationalSymposium on Electromagnetic Compatibility, 2004*, Institute of Electrical and Electronics Engineers (IEEE), Jan 2004.
The definitive version is available at https://doi.org/10.1109/ISEMC.2004.1349988

Using Near-Field Scanning to Predict Radiated Fields

Jin Shi, Michael A.Cracraft , Jianmin Zhang
Richard E. DuBroff

Electromagnetic Compatibility Laboratory
Department of Electrical and Computer Engineering
University of Missouri - Rolla
Rolla, MO 65409
Email: shi@umr.edu; cracraft@umr.edu;
jzp4f@umr.edu;red@ece.umr.edu;

Kevin Slattery
Intel Corporation, Hillsboro, OR
Email: kevin.p.slattery@intel.com

Masahiro Yamaguchi
Department of Electrical and Communication Engineering
Tohoku University
Sendai, Japan
E-mail: yamaguti@ecei.tohoku.ac.jp

Abstract— **Near-field scanning has often been used to measure and characterize magnetic fields surrounding individual integrated circuits (IC) and high speed digital electronic circuits. The objective of the work described herein is to use near-field scanning data, performed in a typical laboratory bench top environment, to predict radiated electromagnetic interference (EMI) in a typical product environment. The product environment may include enclosures and apertures.**

Keywords- Near-field, EMI, equivalent current

I. INTRODUCTION

The approach described herein begins by acquiring sufficient near-field scanning data to allow representation of an unintentional radiating source (e.g. an IC chip) by an equivalent surface current distribution. The use of equivalent current distributions to represent sources is well known [1,2]. As a recent example, Sarkar and co-workers [3,4,5] have presented a detailed description of near-field to near/far-field transformations for an arbitrary near-field geometry by introducing an equivalent electric or magnetic current source.

In the present work, the equivalent current distribution is used as a source in numerical full wave modeling. This modeling may include additional objects that were not present at the time the near-field measurements were made in the laboratory bench top environment. To the extent that mutual interactions between additional objects and the equivalent current source are negligible the predicted field patterns for some simple well characterized radiating structures are often quite comparable to the results of pure simulations— simulations that model the relevant source geometry directly rather than relying on experimentally determined equivalent source currents.

II. BASIC THEORY OF THE EQUIVALENT CURRENT APPROACH

For a collection of intentional or unintentional sources in the region $z \leq z_0$, the magnetic field intensity and its plane wave spectrum can be related through [6-9]:

$$\vec{H}(\vec{r}) = \frac{1}{2\pi} \int_{-\infty}^{+\infty} \int_{-\infty}^{+\infty} \vec{T}_0(k_x, k_y) \cdot e^{i\vec{k}\cdot\vec{r}} dk_x dk_y, z \geq z_0 \quad (1)$$

$$\vec{T}_0(k_x, k_y) = \frac{e^{-i\gamma z}}{2\pi} \int_{-\infty}^{+\infty} \int_{-\infty}^{+\infty} \vec{H}(\vec{r}) e^{-i(k_x x + k_y y)} dx dy, z \geq z_0 \quad (2)$$

where $\vec{k} = k_x \hat{x} + k_y \hat{y} + \gamma \hat{z}$ and

$$\gamma = \begin{cases} \sqrt{\omega^2 \mu\varepsilon - k_x^2 - k_y^2}, & \text{for } k_x^2 + k_y^2 \leq \omega^2\mu\varepsilon \\ i\sqrt{k_x^2 + k_y^2 - \omega^2\mu\varepsilon}, & \text{for } k_x^2 + k_y^2 > \omega^2\mu\varepsilon \end{cases}$$

Use of the plane wave spectrum, $\vec{T}_0(k_x, k_y)$, to calibrate or compensate the probe measurements is described in [10]. Once the probe measurements have been properly compensated, the magnetic field for $z \geq z_0$ can be written in terms of the magnetic field on z_0 [3,4,5] through

$$\vec{H}(\vec{r}) = \nabla \times \int_{-\infty}^{+\infty} \int J_s(\vec{r}') G_0(\vec{r}|\vec{r}') dx' dy' \quad (3)$$

where

$$\vec{J}_s(\vec{r}') = 2\hat{z} \times \vec{H}(\vec{r}')|_{z=z_0}$$

and $G_0(\vec{r}|\vec{r}')$ is the free-space scalar Green's function.

III. NEAR-FIELD MEASUREMENT AND NUMERICAL SIMULATION PROCEDURES

The equivalent current approach consists of two major steps. The first step determines an equivalent surface current distribution from near-field scanning measurement data. The second step predicts the near- and far-field from numerical simulations with the original radiating antenna replaced by the equivalent current and nearby near-field geometries included.

A near-field scanning system typically consists of a test bench, a computer-controlled xyz-positioner, near-field measurement probes and measurement instrumentation. A computer controlled xyz-positioner moves the probe over a pre-selected scan surface, which is in the near-field of the DUT. A vector network analyzer (VNA) or a digital

oscilloscope could be used for measurements containing phase information .The near-field measurement data are recorded in the computer and subsequently analyzed to determine an equivalent current.

Once determined from the measurement data, this equivalent current can replace the original radiating antenna in an FDTD simulation that may include additional nearby objects. A pseudo-wire array is used to incorporate the equivalent surface current distribution as a source in the FDTD code. Every pseudo wire is associated with a sinusoidal source whose frequency, amplitude and initial phase are specified by the corresponding equivalent surface current distribution. The spacing between pseudo-wires is determined by the pre-selected near-field scanning interval. An example of a pseudo-wire array is shown in Figure 1. The horizontal arrows parallel to the x-axis represent J_x and the vertical arrows parallel to the y-axis represent J_y.
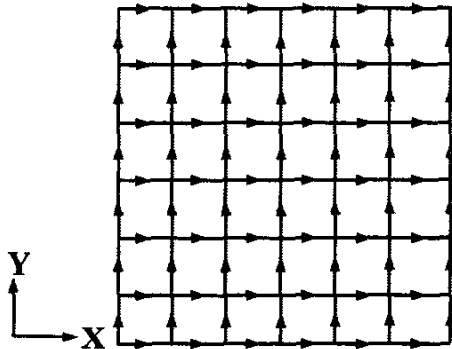

Figure 1. A grid of the pseudo wires to model the equivalent surface current source

IV. EXPERIMENTAL AND NUMERICAL RESULTS

A microstrip structure was chosen as a DUT in this case. The objective is to predict the magnetic field when a nearby conducting object is introduced. The geometry of this microstrip is shown in Figure 2. The trace shown in Figure 2 is 20 mm long by 2 mm wide and the circuit board is 75 mm along each edge. As shown in Figure 2, the trace is fed at one end and terminated in a 50 Ohm load at the other end. The nearby conducting object is chosen as a 25mm x 25mm square copper sheet to model a square perfect electric conductor (PEC).
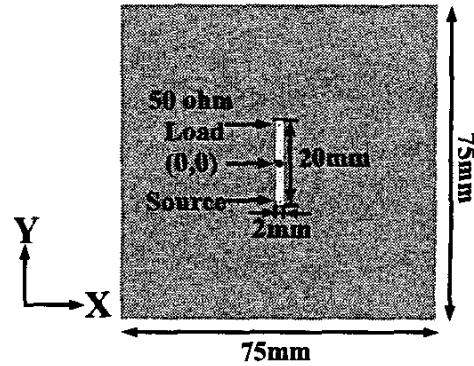

Figure 2. Front view of a microstrip structure

Figure 3 shows a photograph of the near-field measurement setup. For the determination of the equivalent current, the near-field measurement will be conducted without the presence of the square PEC shown in Figure 3. Figure 4 shows the definitions of two different scan planes. The scan planes were defined as square planes, with dimensions of 76.5mm and 76.5 mm, parallel to the microstrip plane. The center of each scan plane and the center of the microstrip ground plane were set to coincide. Data obtained from near-field scanning on plane 1 was used to determine the equivalent current distribution. The equivalent current distribution was then used to predict the magnetic field on plane 2 when the PEC was present. Near-field scan measurements were also performed on plane 2 and used to corroborate the predictions.

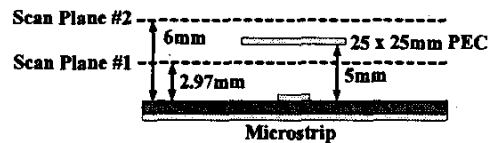Figure 3. Side view of the measurement setup

Figure 4. Definition of planes for equivalent current source determination and magnetic field comparison (From a side view)

The near-field radiation generated by the microstrip structure will be compared between full wave simulations and

VNA measurements. Relevant procedural steps for comparing near-field radiation are summarized in Figure 5. More specifically, the near-field radiation comparison in this case refers to the magnetic field comparison.

According to this procedure, near-field scan measurements were performed on scan plane 1 first to determine the equivalent electric current sources. This includes two main steps. The first step is a probe calibration and compensation technique [10]. A set of near-field measurements is performed by running an uncalibrated probe over a well characterized antenna. The measurements are then used to characterize the relation between the probe output and the field. The characterization yields a 2 row by 3 column matrix in which each element is a function of frequency and wave-number. Once this characterization has been obtained, the previously uncalibrated probe can be used to make measurements of the microstrip on the bench top of the near-field scanning system. The probe effects can then be compensated and thereby removed from these measurements to yield estimates of the magnetic and/or electric fields.

From estimates of the magnetic field, for example, a set of equivalent current sources can be derived and used in an FDTD numerical simulation that includes a 25 mm by 25 mm PEC not present when the near-field scan measurements were made. Based on these experimentally determined equivalent sources, the FDTD simulation can make some prediction of the radiation produced by the microstrip in a more realistic environment that may include additional scattering objects.

To provide experimental validation of the results from this simulation, a new set of near-field scan measurements were performed on plane 2. This time the measurement configuration as shown in Figure 3 included a layer of copper tape on a Styrofoam block to mimic the PEC used in the numerical simulation. An independent FDTD simulation, incorporating a microstrip model and a square sheet PEC model, provides a reference of the near-field distribution on plane 2. Figure 5 shows the relevant procedural steps for comparing near-field radiation.
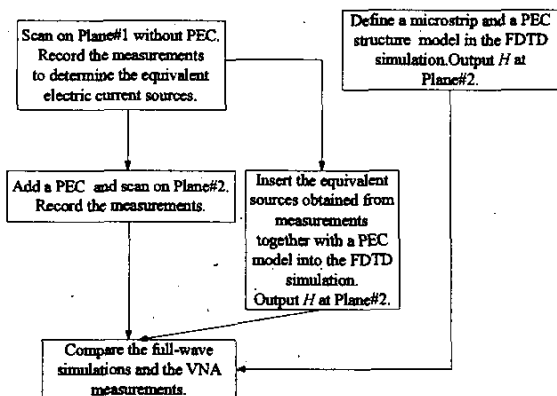
During the process of near-field scanning measurements, the microstrip structure was driven through port 1 of an HP8753D vector network analyzer. A small loop magnetic field probe was mounted on a computer controlled positioner to scan over planes 1 and 2. The probe output was connected to port 2 of the VNA. The microstrip was set in the center of the scan area. The probe was moved over a scan area divided into 51 by 51 intervals with each interval set at a width of 1.5mm.

Measured and simulated results are displayed for a frequency of 100 MHz in Figure 6. Figure 6a shows near-field measurements conducted on scan plane 2 (6mm above the microstrip, with a 25mm x 25mm PEC set 5mm above microstrip). The first and the second panel in Figure 6a correspond to the amplitudes of the probe outputs (S_{21}) when the normal direction of the probe loop was set parallel to the x and y axes respectively.

Figure 6b shows an independent FDTD simulation on plane 2, which incorporates a microstrip model and a PEC sheet model. Figure 6c also shows an FDTD simulation result on plane 2. However in this case, the excitation was provided by the equivalent electric current source which, in turn, was based on near-field measurements made in the absence of the additional PEC region. Rescaling was done on all plots to normalize them on a zero to one linear scale.
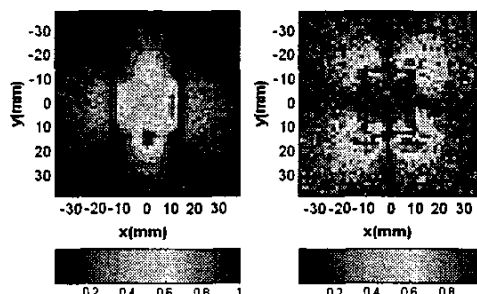
(a). $|S_{21}|$ for probes oriented in the x and y directions
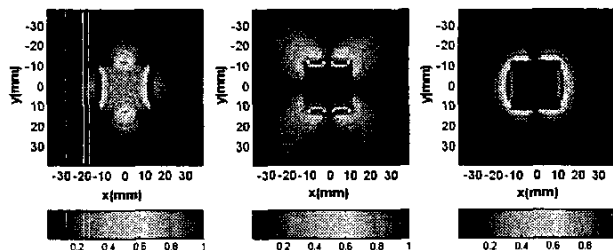
(b). Magnitude of the magnetic field components in the x, y, and z directions predicted by an FDTD simulation incorporating a microstrip and a PEC sheet model

Figure 5. Procedures of near-field (magnetic field) prediction comparison on plane 2

16
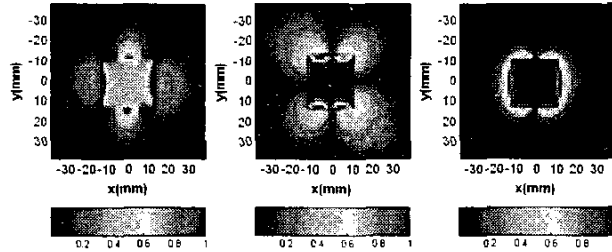
(c). Magnitude of the magnetic field components in the x, y, and z directions predicted by an FDTD simulation incorporating the equivalent current source and a PEC sheet model

Figure 6. A comparison of magnetic fields measured, simulated and simulated based on near-field measurements on plane 2 (Rescaling was done on all plots to normalize them on a zero to one linear scale.)

The results shown in this figure indicate at least qualitative agreement between the full wave simulation results and near-field measurements. The patterns are quite similar, although Figure 6a (direct measurements) appears rather noisy. This may be due to the imperfect performance of the probe and the limited output power level of the network analyzer. The agreement between the full wave simulation results and near-field measurements shows that the radiating microstrip structure could be replaced with an equivalent current source residing on a fictitious surface. Another limitation might be caused by multiple interactions between nearby scattering objects and the excitation source. These multiple interactions are considered to be minor in this example and are not properly accounted for in the equivalent source model used so far.

A more detailed comparison can be obtained from various cuts through the plots shown in Figure 6. For example, along the line y=0, the plots in the leftmost column of Figure 6a, b and c can be redrawn as ordinary line plots as shown in Figure 7. Similar comparisons can be made for the same column of Figure 6a, b and c by considering the cut through the line x=0 and for the third column of Figure 6b and c along the line y=0. These two comparisons are shown in Figure 8 and Figure 9 respectively.
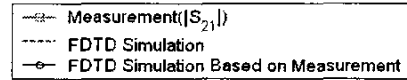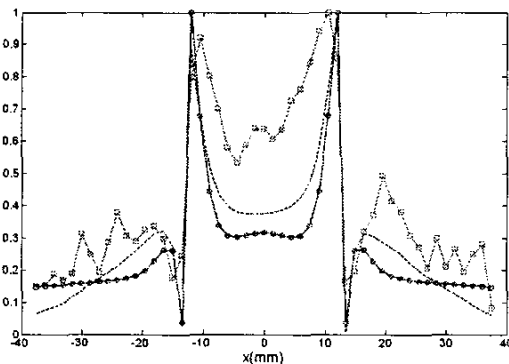

Figure 7. A comparison of the output for a probe ($|S_{21}|$) oriented in the x direction, the magnitude of Hx predicted from an FDTD simulation incorporating a microstrip model with a PEC sheet model; and the magnitude of Hx predicted from an FDTD simulation incorporating an equivalent current and a PEC sheet model. The y coordinate in this graph was fixed at 0.
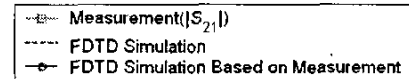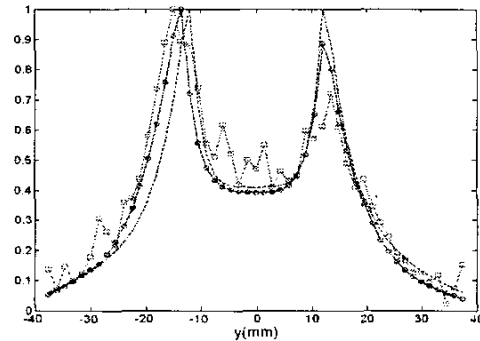

Figure 8. A comparison of the output for a probe ($|S_{21}|$) oriented in the x direction, the magnitude of Hx predicted from an FDTD simulation incorporating a microstrip model and a PEC sheet model; and the magnitude of Hx predicted from an FDTD simulation incorporating an equivalent current and a PEC sheet model. The x coordinate in this graph was fixed at 0.
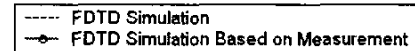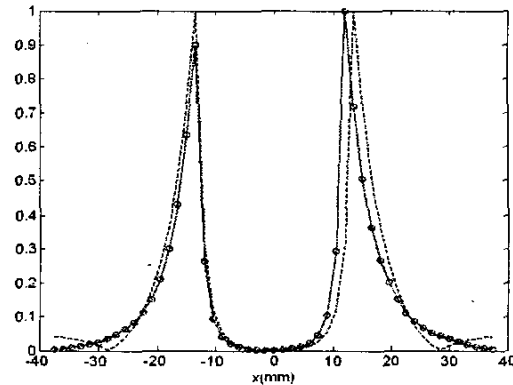

Figure 9. A comparison of the magnitude of H_z predicted from an FDTD simulation incorporating a microstrip model and a PEC sheet model; and the magnitude of H_z predicted from an FDTD simulation incorporating an equivalent current and a PEC sheet model. The y coordinate in this graph was fixed at 0.

V. SUMMARY AND CONCLUSIONS

A procedure was presented in this paper for an application of an equivalent current approach to the problem of characterizing radiated EMI that may include enclosures with apertures and nearby conducting objects through the use of near-field scanning measurements. The agreement between direct full wave simulation results and full wave simulation results using equivalent sources works well under certain assumptions.

REFERENCES

[1] Robert S. Elliott, Antenna Theory and Design, Englewood Cliffs, NJ: Prentice Hall, 1981, Chapter 1.

[2] Constantine A. Balanis, Advanced Engineering Electromagnetics, New York: John Wiley & Sons, 1989, Chapter 7.

[3] Tapan Kumar Sarkar, and Ardalan Taaghol, "Near-field to near/far-field transformation for arbitrary near-field geometry utilizing an equivalent electrical current and MoM ", IEEE Trans. Antennas Propagat., vol.47, no.3, pp.566-573, March, 1999

[4] Peter Petre and Tapan K. Sarkar, "Planar near-field to far-field transformation using an equivalent magnetic current approach", IEEE Trans. Antennas Propagat., vol.40, no.11, pp.1348-1356, November, 1992

[5] Ardalan Taaghol and Tapan K. Sarkar, "Near-field to near/far-field transformation for arbitrary near-field geometry utilizing an equivalent magnetic current", IEEE Trans.Electromagn. Compat., vol.38, no.3, pp.536-542, August, 1996

[6] D.T. Paris, W. M. Leach and E.B. Joy, "Basic theory of probe-compensated near-field measurements ", IEEE Trans. Antennas Propagat., vol.AP-26, no.3, pp.373-389, May, 1978

[7] Thorkild B. Hansen and Arthur D. Yaghjian, Plane-Wave Theory of Time-Domain Fields. Piscataway, NJ: IEEE Press, 1999.

[8] T. B. Hansen and A. D. Yaghjian, "Formulation of probe-corrected planar near-field scanning in the time domain", IEEE Trans. Antennas Propagat., vol.43, no.6, pp.569-584, June, 1995

[9] Glenn S. Smith, An Introduction to Classical Electromagnetic Radiation.

Cambridge, United Kingdom: Cambridge University Press, 1997, ch.4, pp.262-272

[10] Jin Shi, M.A. Cracraft, K. P. Slattery, Masahiro Yamaguchi and R.E. DuBroff, "Calibration and compensation of near-field scan measurements for EMI characterization", IEEE Trans. Electromagn. Compat., submitted for publication